Strengthening mechanisms of Ti via Al addition

L. Bolzoni*, S. Raynova, F. Yang

Waikato Centre for Advanced Materials and Manufacturing, School of Engineering, The University of Waikato, Hamilton 3240, New Zealand

*Corresponding author. Tel. +64 7 8379381 Fax. +64 7 8384835

E-mail address: bolzoni.leandro@gmail.com (L. Bolzoni).

Abstract

Pure Ti is characterised by an interesting combination of performance from an engineering point of view. The addition of Al to Ti can be used to reduce the intrinsic cost of the material, decrease the density of the alloy, and increase the mechanical performance. This study is focused on evaluating the physical properties, microstructural evolution and mechanical behaviour of Ti-xAl alloys (where x = 1-6 wt.%) in order to scientifically understand the strengthening mechanisms of the addition of Al to pure Ti manufactured via the conventional powder metallurgy route of cold uniaxial pressing plus solid state sintering. The addition of Al to Ti does not affect the compressibility of the alloy but changes the consolidation and densification of the alloy. The incremental addition of Al results in the progressive strengthening of Ti via the simultaneous contribution from substitutional solid solution and grain refinement strengthening which outdo the negative effect of the residual porosity.

Keywords: low-cost titanium alloy, titanium powder metallurgy, press and sinter, blending elemental, homogeneous microstructure, strengthening

1. Introduction

The combination of properties that Ti can provide for engineering applications include low density, which is approximately 50% that of nickel, passivity which leads to excellent corrosion resistance and biocompatibility with human body fluids, high strength (which is also maintained up to relatively high temperatures), and high specific properties (i.e. mechanical performance in relation to the density) [1, 2]. More in details, the mechanical behaviour of pure Ti is significantly affected by the presence of interstitial elements where oxygen and nitrogen have the highest impact [3, 4]. In particular, the residual amount of oxygen left by the extractive metallurgy process used to obtain pure Ti in its metallic form is used to classify Ti into four different commercially pure (CP) Ti grades [5]. CP Ti is therefore used in application where high corrosion resistance and good strength are needed such as for non-structural aircraft parts, chemical and marine applications, heat exchangers, and components for chemical processing and desalination equipment [6].

The mechanical behaviour of Ti can also be changed via alloying (i.e. substitutional strengthening). Specifically, as Ti is characterised by an allotropic phase transformation, alloying elements can be used to stabilise the low temperature HCP α-Ti phase or the high temperature BCC β-Ti phase. These alloying elements are thus divided depending on their stabilising effect into α and β stabilisers. Oxygen, nitrogen and Al are all α stabilisers but, generally, only the latter is intentionally added as an alloying element and the others are present as impurities. In particular, the addition of Al is highly desirable as Al is cheaper than Ti, is lighter than Ti, allows to maintain higher deformability with respect to the addition of other α stabilisers, and increases the oxidation resistance of Ti at high temperatures. Nevertheless, in Ti alloys, the maximum amount of Al is generally kept below 6-7 wt.% to prevent the formation of the Ti_3Al intermetallic compound (known as α_2) which embrittles the material [7, 8].

Reduction of the intrinsic cost of Ti is an active field of research [9-11], because Ti is more expensive with respect to competitor metals such Al and Fe due to its high affinity for interstitials (which makes its extraction and casting costly), and high poor machinability (which makes its shaping difficult). The addition of cheaper elements and the use of creative fabrication methods such as powder metallurgy (PM) [14] are among the different alternatives available to decrease the final manufacturing costs of titanium products. Particularly, PM methods have the intrinsic advantages of being near-net-shape techniques [15] characterised by high material's yield where both aspects are very important for an expensive metal such as Ti. Conventional [16-18] and alternative [19, 20] powder metallurgy methods have been investigated to obtain dense and porous titanium products [16, 21] where α+β alloys are the most studied [22-25]. The aim of this investigation is therefore to understand the effect of the addition of a progressively higher amount of Al (to reduce the intrinsic cost of the material) to Ti produced via cold pressing plus solid state sintering, the cheapest of the PM technique, to limit the manufacturing costs.

2. Experimental procedure

The base material for the investigation was an irregular HDH (hydride-dehydride) Ti powder with particle size lower than 75 μm and oxygen content of 0.3 wt.%. The atomised aluminium powder used was spherical in morphology with maximum particle size of 45 μm. The correct amount of each powder was weighted and mixed during 25 min in a V-shaped blender at 45 rpm to achieve homogeneous blends of Ti-xAl powders, where x = 1-6 wt.%, using the blending elemental approach. Samples were therefore labelled accordingly. The powder mixtures were then uniaxially warm pressed (120±10°C) into 40 mm diameter samples using a cylindrical die whose walls were lubricated with graphite and applying 600 MPa maintaining the maximum pressure for 1 min. The samples were subsequently

consolidated via vacuum sintering (heating rate of 10ºC/min) at 1250ºC during 2 hours prior to furnace cooling.

The dimensions and weight of the green samples were measured, respectively, using a 2-decimal digital calliper and a high precision analytical scale, and the values used to calculate the green density as mass/volume ratio. The values of the density of the sintered samples were quantified via water displacement measurements. The theoretical density of samples was calculated using the rule of the mixture, using the Ti (4.51 g/cm^3) and Al (2.70 g/cm^3) theoretical density values, to be able to calculate relative density values. Quantification of the consolidation induced by the sintering process was done via the densification parameter [26]. The classical metallographic route (i.e. grinding and polishing) was used to prepare the sample for microstructural analysis, samples which were chemically etched by means of a Kroll reagent (2 ml HF, 6 ml HNO_3, and 92 ml distilled water). Optical micrographs were captured with a Nikon digital camera attached to an Olympus BX60F5 microscope. X-ray diffraction (XRD) analysis was carried out using a Philips X'Pert diffractometer using scan step size of 0.013º in the 30-80º 2-Theta range. Dog-bone tensile test-pieces with rectangular cross section of 2x2 mm^2 and gauge length of 20 mm were cut via EDM (electrical discharge machining) and ground with SiC grinding papers to eliminate any potential influence from the cutting operation. Tensile tests were done on an Instron 33R4204 machine using a cross head speed of 0.1 mm/min and an external mechanical extensometer was used to measure the elongation of the samples. The yield strength of the sintered materials was calculated via the offset method. Rockwell hardness (HRA) measurements were used to quantify the hardness of the materials. It is worth mentioning that for the mechanical characterisation a minimum of five measurements were performed. Fractographic analysis of the broken dog-bone tensile test-pieces was performed via a Hitachi S4700 SEM.

3. Results

Figure 1 shows the variation of the relative densities (before and after sintering) for different amount of Al added to Ti where it can be seen that the green density is fairly constant whilst there is a slight increment in the values from Ti-1Al to Ti-2Al and afterward the density of the sintered samples decreases with the Al content. Coherently, the densification of the alloys initially increases with the addition of Al but then progressively decreases starting from an addition rate of 3 wt.% of Al.

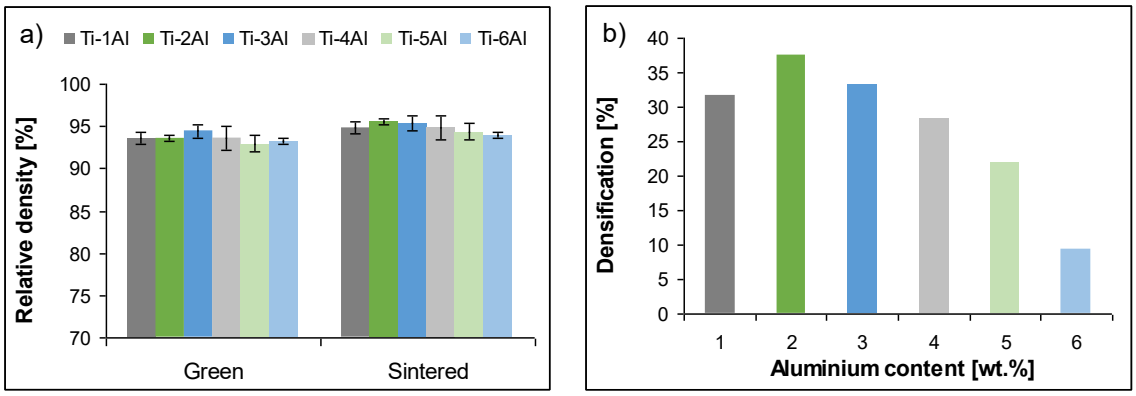

Figure 1. Variation of the physical properties of the sintered Ti-xAl alloys: a) green and sintered density, and b) densification parameters vs Al content.

Representative optical micrographs of the Ti-xAl alloys showing the size, shape and distribution of the residual porosity as well as the morphology of the grains are shown in Figure 2. Spherical pores are present in every material but the size and percentage increase with the addition of Al, which also leads to the formation of coarse α-Ti lamellae which are the main microstructural phase of the sintered Ti-xAl alloys as seen both at low and high magnification.

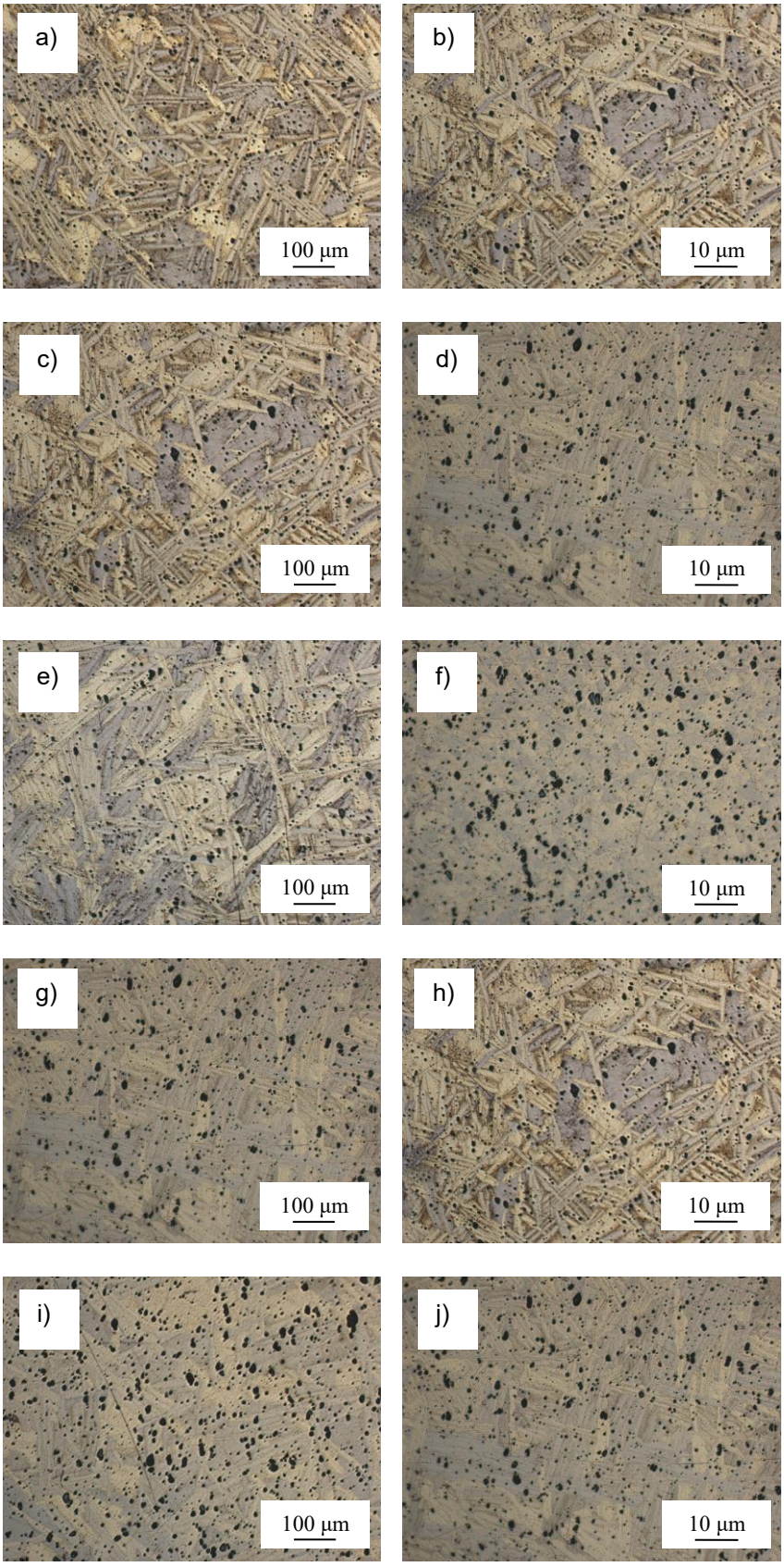
a)
100 µm
b)
10 µm
c)
100 µm
d)
10 µm
e)
100 µm
f)
10 µm
g)
100 µm
h)
10 µm
i)
100 µm
j)
10 µm

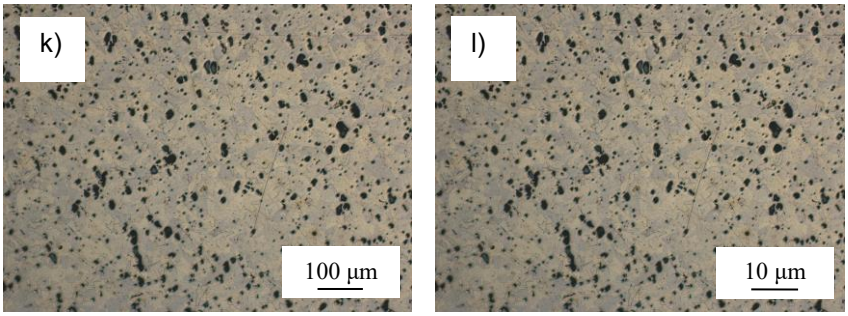

Figure 2. Representative optical micrographs (low and high magnification, respectively) of the sintered Ti-xAl alloys: a-b) Ti-1Al, c-d) Ti-2Al, e-f) Ti-3Al, g-h) Ti-4Al, i-j) Ti-5Al, and k-l) Ti-6Al.

The size of the lamellae as well as that of the prior β grains progressively changes with the Al content but the most significant change is found for an Al content of 6 wt.% which could be due to the precipitation of other phases, where the most probable is the α_2 phase [7, 8]. Therefore, XRD analysis of the Ti-6Al alloy was carried out with the aim of identifying the phases present and the related XRD pattern is shown in Figure 3 where it can be seen that only peaks corresponding to the α-Ti phase were detected.

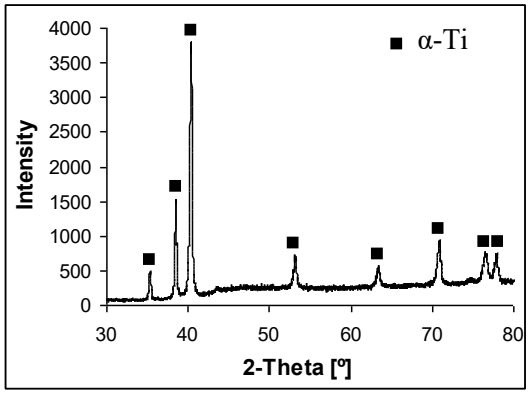

Figure 3. XRD pattern of the sintered Ti-6Al alloy.

Figure 4 and Figure 5 show, respectively, representative examples of the stress-strain behaviour and the average quasi-static tensile properties (i.e. yield and ultimate tensile

strengths, and ductility) of the Ti-xAl alloys. It is found that the Ti-xAl alloys are characterised by both elastic and plastic behaviour regardless of the total amount of Al added which leads to the progressive increment of the strength but also to a parabolic trend of the ductility of the alloy.

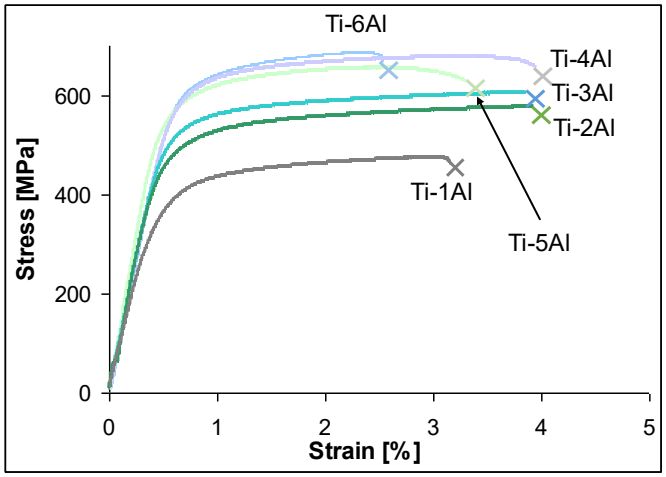

Figure 4. Representative stress-strain curves of the sintered Ti-xAl alloy.

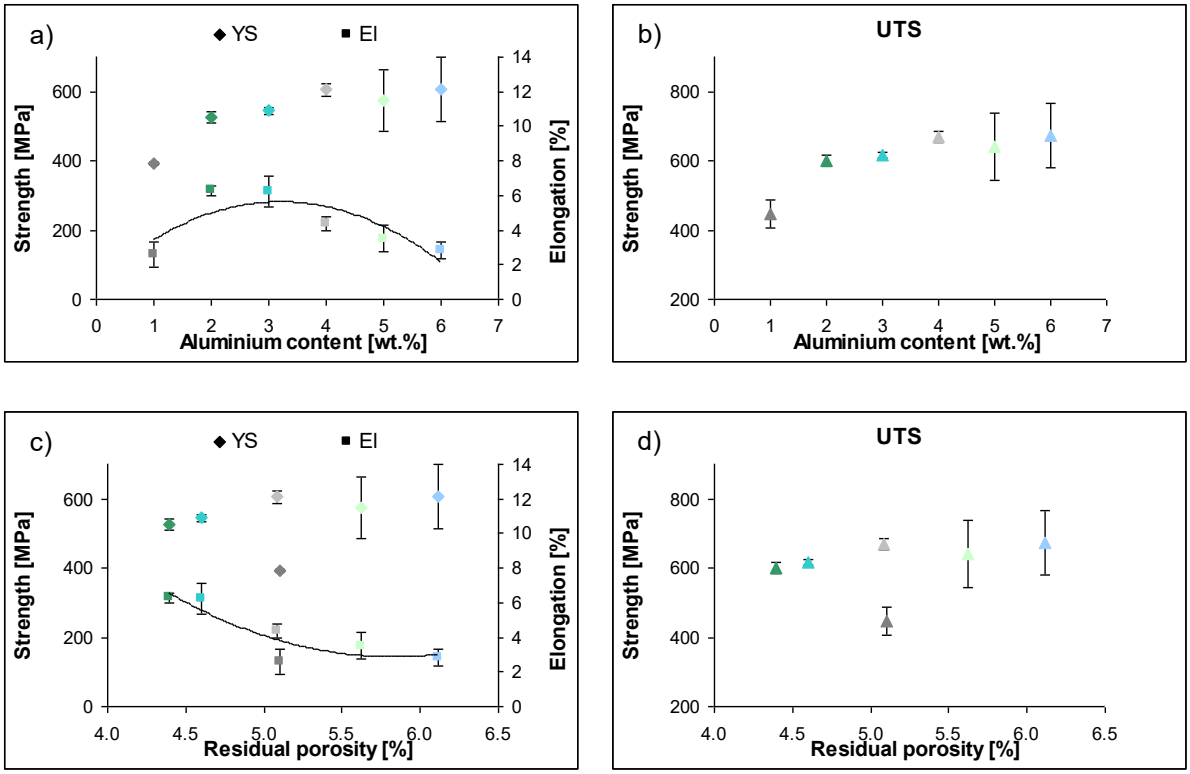

Figure 5. Variation of the average quasi-static tensile properties of the sintered Ti-xAl alloys: a) yield strength and elongation vs Al content, b) ultimate tensile strength vs Al content, c)

yield strength and elongation vs residual porosity, and d) ultimate tensile strength vs residual porosity.

Figure 6 shows the fractographic analysis of the binary Ti-xAl sintered samples where it can be seen that the materials are characterized by the presence of several dimples, typical of ductile behaviour of metals, in agreement with the stress-strain curves of Figure 4. Specifically, dimples are the main features of binary Ti-xAl alloys with Al content of 2-3 wt.%, composition from which tear ridges starts to appear; this is associated with the decrement of the ductility of the material. Moreover, the cleavage fracture of metals with a H.C.P. lattice and cleavage facets (i.e. transgranular fracture) are also found in the fracture surface of the Ti-1Al and Ti-6Al alloys due to their lower ductility.

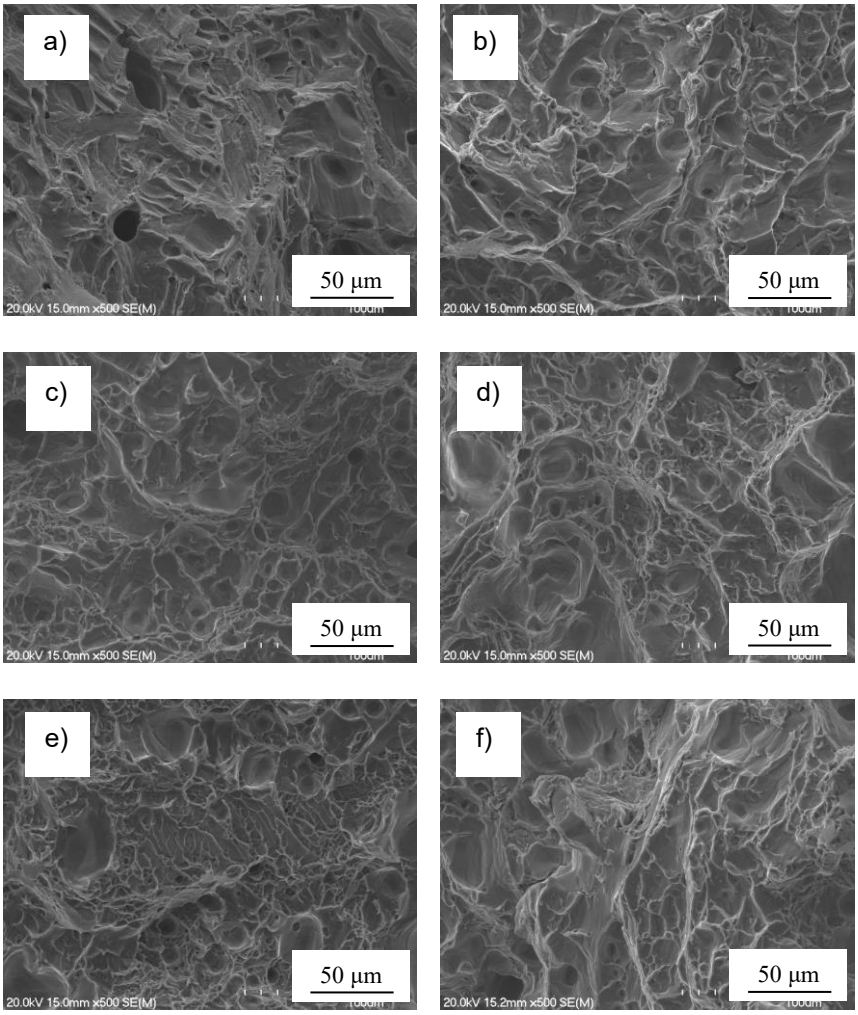

Figure 6. Representative SEM fractographic images of the sintered Ti-xAl alloys: a) Ti-1Al, b) Ti-2Al, c) Ti-3Al, d) Ti-4Al, e) Ti-5Al, and f) Ti-6Al.

The variation of the hardness of the sintered Ti-xAl alloys with the Al content is shown in Figure 7 where it can be seen that, conversely to what it could be expected from the classical powder metallurgy theory [27, 28], the material becomes progressively harder as the Al content increases although the residual porosity increases with the Al content.

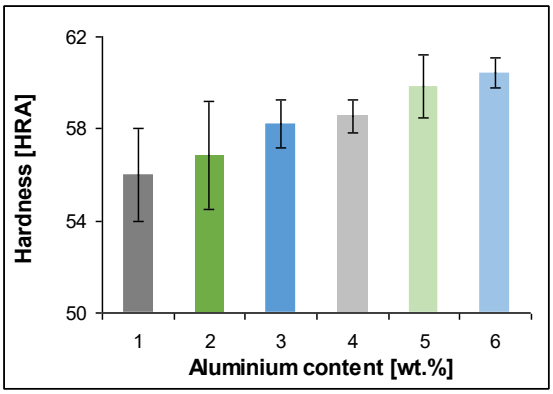

Figure 7. Variation of the hardness of the sintered Ti-xAl alloys with the Al content.

4. Discussion

Analysis of the relative density data (Figure 1) indicates that the addition of the spherical Al powder particles does not affected, or at least not significantly, the compressibility of the alloy as the green density remains almost constant with the increment of the Al content. This is due to the combination of two factors: the higher deformability of the Al powder particles and the difference in terms of particle size distribution. However, it is found that the addition of Al changes the thermodynamics of the sintering process where the initial addition of Al to Ti induces an increment of the relative density for an Al content of up to 2 wt.%. A further addition of Al actually leads to a continuous decrement of the values of the relative density of the sintered samples. Coherently with the trend of the relative density, the densification of the

Ti-xAl alloys reaches its maximum for the Ti-2Al alloy and subsequently decreases. It is known that the initial melting of Al induces some swelling of the samples starting from 660ºC due to the formation of the Al_3Ti intermetallic compound in the surface of the Ti particles. The process actually starts below the melting of Al due to the higher intrinsic diffusivity of Al (compared to Ti [29, 30]) but the melting of Al leads to wetting of the Ti powder particles and penetration of the liquid Al between the Ti particles by capillarity forces and thus to the rapid formation of complete coating of Al_3Ti layers on the Ti powder particles. The associated formation of large pores having low activity for the subsequent solid state sintering is driven by the redistribution of the molten Al. Continuation of the reaction until the complete consumption of the Al melt and the increase of the thermodynamic energy of the system as consequence of the increase of the temperature during the heating stage of sintering results in the disintegration of the Al_3Ti coating layer into single Al_3Ti grains surrounding the Ti powder particles [31]. Eventually the spherical Al_3Ti grains go into solution during the prolonged sintering cycle. However, the Kirkendall porosity left by the fast diffusing Al into the Ti lattice leaves behind porosity that cannot be completely recover during the pressureless sintering process.

In agreement with the relative density data, the sintered Ti-xAl samples are all characterised by the presence of residual porosity where the amount of porosity and its size increase with the increment of the Al content but its distribution is homogeneous through the microstructure regardless of the alloy composition. The porosity is primarily isolated and spherical in shape, indicating that with the sintering parameters employed the materials reached the third stage of sintering; however, interconnected porosity, due to the coalescence of isolated pores during the last stage of sintering, starts to appear for Ti-xAl alloys with an Al content equal or greater than 5 wt.%. This is due to the fact that the materials were sintered at the same temperature which is, as per the binary Ti-Al phase diagram [32],

progressively closer to the β transus of the alloy. The microstructure of sintered Ti is characterised by equiaxed α-Ti grains whose size depends on the particle size of the powder used and on the parameter utilised to sinter the material [17]. However, from Figure 2 it can be seen that the addition of Al to Ti leads to the formation of microstructures constituted by α-Ti lamellae. Specifically, the initial addition leads to a very coarse microstructure which is progressively refined as the amount of Al present in the Ti-xAl alloys increases. More in details, a minority of quasi-equiaxed α-Ti grains is still present in the Ti-1Al and Ti-2Al alloys but which completely transform into needle-shaped grains starting from an Al content of 3 wt.%. Interestingly, the size of the prior β grains increases with the Al content. However, a much finer microstructural features are found in the Ti-6Al alloys which is composed of fine α-Ti lamellae within much finer prior β grains. Overall, the resulting microstructure is a coarse platelet Widmanstätten type structure [33]. The phases present in the Ti-xAl alloys were detected via XRD analysis and, as demonstrated via the results of the XRD pattern of the Ti-6Al alloy (Figure 3), only peaks of the α-Ti phase are found. It is worth mentioning that the position of the peaks is shifted toward slightly higher diffraction angles in comparison to CP Ti due to the presence of substitutional Al atoms within the HCP α-Ti lattice and, if the precipitation of the α_2 phase occurred, its amount is below the detection limit of the equipment used. In particular, Al has a smaller atomic radius in comparison to Ti and thus its substitution of Ti atoms leads to the distortion of the α-Ti lattice. As per Bragg's law, the shift is associated with the reduction of the interatomic plane distance [34].

From the quantification of the tensile behaviour of the sintered Ti-xAl alloys it is found that they have comparable modulus of elasticity, as the stress-strain curves of Figure 4 overlap, and they deform plastically prior to fracture but there is a significant strengthening effect induced by the addition of Al which shifts to progressively higher values the applied load at which the alloy switches from elastic to plastic deformation. More specifically, both the yield

strength and the ultimate tensile strength increase continuously with the Al content (Figure 5) due to the simultaneous contribution of the substitutional strengthening effect of the presence of the Al atoms in the HCP α-Ti lattice and the progressive refinement of the microstructural phases that compose the Ti-xAl alloys (Figure 2). It is clear that the combined solid solution and grain refinement strengthening overcome the effect of the increased amount of residual porosity left by the sintering stage as the strength increases continuously with the addition of Al. The same factors (i.e. solid solution and grain refinement) are also the responsible for the progressive increase in hardness of the material with the increment of the Al content (Figure 7). Once again both aspects contributing to the hardening of the Ti-xAl alloys overcome the negative effect that the residual porosity would have on the hardness of pressureless sintered materials, where the hardness is expected to decrease with the increment of the residual porosity [27]. Regarding the ductility of the Ti-xAl alloys, it is found that the elongation to fracture initially increases with the Al content but then starts to decrease for an Al content of 4 wt.% leading to a parabolic trend (Figure 5a). In this case, the ductility of the sintered Ti-xAl alloys is significantly affected by the increasing amount of residual porosity (as pores act as stress concentration sites) and therefore an exponential decreasing trend of the elongation to fracture with the residual porosity is found (Figure 5c). Apart from the effect of the residual porosity, the ductility of the Ti-xAl alloys is also affected by the strengthening effects as ductility and strength are mutually exclusive properties and consequently the fracture surface of the material switches from being primarily composed of ductile dimples to a combination of dimples and tear ridges (Figure 6) consistently with the reduction of the ductility. Generally, the properties of the Ti-xAl alloys are higher with respect to wrought CP Ti and comparable to those of the near-α wrought Ti-3Al-2.5V alloy (yield strength = 485 MPa and ultimate tensile strength = 620 MPa) [6]. As Al is much cheaper than Ti, approx. 2.4$/kg vs 12.0$/kg [14] in metal form, the incremental addition of Al substituting Ti in

binary Ti-xAl alloys results in a proportional reduction of the intrinsic cost of the material resulting in a saving of approx. 5% for an addition rate of 6 wt.% of Al. This means that, similarly to Ti-3Al-2.5V, binary Ti-xAl alloys could be employed in non-critical applications such as in tubular form for various aerospace hydraulic and fuel systems, sports equipment, medical and dental implants, reaction vessels, heat exchangers, and electrochemical processing equipment [6]. Optimisation of the manufacturing route, such as hot extrusion to obtain tubular products, could also result in a further improvement of the mechanical performance of the binary Ti-xAl alloys.

5. Conclusions

From this study about the effect of the addition of Al to Ti produced via powder metallurgy to reduce the intrinsic cost of the material, lower the theoretical density of the material and increase the mechanical performance it can be concluded that Al does not affect the processability of the alloy, as the compressibility (green density) remains constant, but Al has a strong effect on the sintering thermodynamics as well as on the stabilisation of the α-Ti phase. Specifically, the incremental addition of Al transforms the microstructure of Ti from equiaxed to coarse platelet Widmanstätten and changes the size and shape of the lamellae, including the interlamellar spacing. The addition of Al results in a progressive strengthening of pure Ti via combined substitutional solid solution and grain boundary strengthening. Consequently, binary Ti-xAl alloys could be used in non-critical aerospace and non-aerospace applications where high performance and reduction of the material cost are of interest.

Acknowledgements

The authors are thankful for the financial support from the New Zealand Ministry of Business, Innovation and Employment (MBIE) through the UOWX1402 research contract. L. Bolzoni would also like to acknowledge the technical support from Mr. Balakrishnan Manogar.

Data Availability

All metadata pertaining to this work will be made available on request.

References

[1] M.J. Donachie, Titanium. A Technical Guide, 2nd Edition ed., ASM International, Ohio, USA, 2000.

[2] C. Leyens, M. Peters, Titanium and Titanium Alloys. Fundamentals and Applications, Wiley-VCH, Köln, Germany, 2003.

[3] F. Geng, M. Niinomi, M. Nakai, Observation of Yielding and Strain Hardening in a Titanium Alloy Having High Oxygen Content, Materials Science and Engineering: A, 528 (2011) 5435-5445.

[4] A. Amherd Hidalgo, R. Frykholm, T. Ebel, F. Pyczak, Powder Metallurgy Strategies to Improve Properties and Processing of Titanium Alloys: A Review, Advanced Engineering Materials, 19 (2017) 1600743.

[5] S.J. Gerdemann, Titanium Process Technologies, Advanced Materials & Processes, 159 (2001) 41-43.

[6] R. Boyer, G. Welsch, E.W. Collings, Materials Properties Handbook: Titanium Alloys, in: A. International (Ed.), Ohio, USA, 1998.

[7] A. Gysler, S. Weissmann, Effect of Order in Ti_3Al Particles and of Temperature on the Deformation Behavior of Age-hardened Ti-Al Alloys, Materials Science and Engineering, 27 (1977) 181-193.

[8] H. Wu, L. Geng, G. Fan, X. Teng, H. Qi, Nanoscale Strain Characterization of Ti_3Al Precipitate-reinforced Ti Alloys, Materials Letters, 209 (2017) 182-184.

[9] D. Agrawal, Microwave Sintering, Brazing And Melting Of Metallic Materials, Sohn International Symposium Advanced Processing of Metals and Materials Volume 4 - New, Improved And Existing Technologies: Non-Ferrous Materials Extraction and Processing, (2006).

[10] L. Bolzoni, E.M. Ruiz-Navas, E. Gordo, Influence of Sintering Parameters on the Properties of Powder Metallurgy Ti-3Al-2.5V Alloy, Materials Characterization, 84 (2013) 48-57.

[11] C.S. Wang, K.S. Zhang, H.J. Pang, Y.Z. Chen, C. Dong, Laser-induced Self-propagating Reaction Synthesis of Ti-Fe Alloys, Journal of Materials Science, 43 (2008) 218-221.

[12] S.H. Hong, Y.J. Hwang, S.W. Park, C.H. Park, J.-T. Yeom, J.M. Park, K.B. Kim, Low-cost Beta Titanium Cast Alloys with Good Tensile Properties Developed with Addition of Commercial Material, Journal of Alloys and Compounds, 792 (2019) 271-276.

[13] Y.J. Hwang, S.H. Hong, Y.S. Kim, H.J. Park, Y.B. Jeong, J.T. Kim, K.B. Kim, Influence of Silicon Content on Microstructure and Mechanical Properties of Ti-Cr-Si Alloys, Journal of Alloys and Compounds, 738 (2018) 53-57.

[14] F.H. Froes, M.N. Gungor, M.A. Imam, Cost-affordable Titanium: The Component Fabrication Perspective, JOM, 59 (2007) 28-31.

[15] A.D. Romig, M.J. DeHaemer, ASM Handbook vol. 7: Powder Metal Technologies and Applications, ASM International, Ohio, USA, 1998.

[16] B.Q. Li, C.Y. Wang, X. Lu, Effect of Pore Structure on the Compressive Property of Porous Ti Produced by Powder Metallurgy Technique, Materials and Design, 50 (2013) 613-619.

[17] L. Bolzoni, E.M. Ruiz-Navas, E. Gordo, Powder Metallurgy CP-Ti Performances: Hydride-dehydride vs. Sponge, Materials and Design, 60 (2014) 226-232.

[18] L. Bolzoni, T. Weissgaerber, B. Kieback, E.M. Ruiz-Navas, E. Gordo, Mechanical Behaviour of Pressed and Sintered CP Ti and Ti-6Al-7Nb Alloy Obtained from Master Alloy Addition Powder, Journal of the Mechanical Behavior of Biomedical Materials, 20 (2013) 149-161.

[19] M. Holm, T. Ebel, M. Dahms, Investigations on Ti-6Al-4V with Gadolinium Addition Fabricated by Metal Injection Moulding, Materials and Design, 51 (2013) 943-948.

[20] L. Bolzoni, E.M. Ruiz-Navas, E. Gordo, Influence of Vacuum Hot-pressing Temperature on the Microstructure and Mechanical Properties of Ti-3Al-2.5V Alloy Obtained by Blended Elemental and Master Alloy Addition Powders, Materials Chemistry and Physics, 137 (2012) 608-616.

[21] N. Jha, D.P. Mondal, J.D. Majumdar, A. Badkul, A.K. Jha, A.K. Khare, Highly Porous Open Cell Ti-foam using NaCl as Temporary Space Holder through Powder Metallurgy Route, Materials and Design, 47 (2013) 810-819.

[22] E. Brandl, F. Palm, V. Michailov, B. Viehweger, C. Leyens, Mechanical Properties of Additive Manufactured Titanium (Ti-6Al-4V) Blocks Deposited by a Solid-state Laser and Wire, Materials and Design, 32 (2011) 4665-4675.

[23] D.F. Khan, H. Yin, H. Li, X. Qu, M. Khan, S. Ali, M.Z. Iqbal, Compaction of Ti-6Al-4V Powder using High Velocity Compaction Technique, Materials and Design, 50 (2013) 479-483.

[24] J. Sun, Y. Yang, D. Wang, Mechanical Properties of a Ti6Al4V Porous Structure Produced by Selective Laser Melting, Materials and Design, 49 (2013) 545-552.

[25] L. Bolzoni, E.M. Ruiz-Navas, E. Gordo, Evaluation of the Mechanical Properties of Powder Metallurgy Ti-6Al-7Nb Alloy, Journal of the Mechanical Behavior of Biomedical Materials, 67 (2017) 110-116.

[26] L. Bolzoni, P.G. Esteban, E.M. Ruiz-Navas, E. Gordo, Mechanical Behaviour of Pressed and Sintered Titanium Alloys Obtained from Prealloyed and Blended Elemental Powders, Journal of the Mechanical Behavior of Biomedical Materials, 14 (2012) 29-38.

[27] R.M. German, Powder Metallurgy Science, 2nd Edition ed., MPIF - Metal Powder Industries Federation, Princeton, USA, 1994.

[28] W. Schatt, K.-P. Wieters, Powder Metallurgy. Processing and Materials, EPMA - European Powder Metallurgy Association, Shrewsbury, UK, 1997.

[29] F.J.J. van Loo, G.D. Rieck, Diffusion in the Titanium-Aluminium System - I. Interdiffusion between Solid Al and Ti or Ti-Al Alloys, Acta Metallurgica, 21 (1973) 61-71.

[30] F.J.J. van Loo, G.D. Rieck, Diffusion in the Titanium-Aluminium System - II. Interdiffusion in the Composition Range between 25 and 100 at.% Ti, Acta Metallurgica, 21 (1973) 73-84.

[31] A. Böhm, B. Kieback, Investigation of Swelling Behaviour of Ti-Al Elemental Powder Mixtures during Reaction Sintering, Zeitschrift für Metallkunde, 89 (1998) 90-95.

[32] J.L. Murray, Phase Diagrams of Binary Titanium Alloys, 1st ed., ASM International, 1987.

[33] G. Steedman, S.F. Corbin, J. O'Flynn, Distinguishing the Influence of Aluminium and Vanadium Additions on Microstructural Evolution and Densification Behaviour during the Sintering of Ti6Al, Ti4V and Ti6Al4V, Powder Metallurgy, 61 (2018) 301-312.

[34] P. Singh, A. Abhash, B.N. Yadav, M. Shafeeq, I.B. Singh, D.P. Mondal, Effect of Milling Time on Powder Characteristics and Mechanical Performance of Ti4wt%Al Alloy, Powder Technology, 342 (2019) 275-287.